Nuclear Instruments and Methods in Physics Research A 613 (2010) 40–45

Contents lists available at ScienceDirect

Nuclear Instruments and Methods in Physics Research A

journal homepage: www.elsevier.com/locate/nima

A dedicated setup for the measurement of the electron transport parameters in gases at large electric fields

P. Fonte [a,b], A. Mangiarotti [a], S. Botelho [c,d], J.A.C. Gonçalves [c,d], M.A. Ridenti [e], C.C. Bueno [c,d,*]

[a] Laboratório de Instrumentação e Física Experimental de Partículas, Departamento de Física da Universidade de Coimbra, 3004-516 Coimbra, Portugal
[b] Instituto Superior de Engenharia de Coimbra, Rua Pedro Nunes, 3030-199 Coimbra, Portugal
[c] Instituto de Pesquisas Energéticas e Nucleares, 05508-000 Cidade Universitária, São Paulo, Brazil
[d] Departamento de Física, Pontificia Universidade Católica de São Paulo, 01303-050 São Paulo, Brazil
[e] Instituto de Física, Universidade de São Paulo, 05508-090 Cidade Universitária, São Paulo, Brazil

ARTICLE INFO

Article history:
Received 30 March 2009
Received in revised form
8 October 2009
Accepted 4 November 2009
Available online 13 November 2009

Keywords:
Electron transport parameters
Drift velocity
First Townsend coefficient
Nitrogen
Isobutane

ABSTRACT

Electron transport parameters are important in several areas ranging from particle detectors to plasma-assisted processing reactors. Nevertheless, especially at high fields strengths and for complex gases, relatively few data are published.

A dedicated setup has been developed to measure the electron drift velocity and the first Townsend coefficient in parallel plate geometry. An RPC-like cell has been adopted to reach high field strengths without the risk of destructive sparks.

The validation data obtained with pure Nitrogen will be presented and compared to a selection of the available literature and to calculations performed with Magboltz 2 version 8.6. The new data collected in pure Isobutane will then be discussed. This is the first time the electron drift velocity in pure Isobutane is measured well into the saturation region. Good agreement is found with expectations from Magboltz.

1. Introduction

Gaseous particle detectors have been, and remain today, a fundamental tool for particle physics and, in general, radiation-based applications. The first modern electronically readout, position-sensitive, large-volume gaseous detector, the Multiwire Proportional Chamber, was introduced by G. Charpak in 1968 and there has been since many new inventions and developments in this field, too numerous to list.

Most gaseous detectors operate in the electron avalanche regime, or beyond, at atmospheric pressure. Their detailed understanding requires, therefore, the knowledge of the electron and ion gas swarm parameters well into the multiplication region, often up to fields of the order of hundreds of Townsend.

Beyond gaseous detectors, swarm parameters are of paramount importance in the modelling of discharge plasmas, since they allow validating electron impact (elastic and inelastic) cross-sections. The latter play a key role in simulating the dynamics of charged particles in plasma-assisted processing reactors, allowing a description of both transport and kinetic features, in view of the monitoring and control of such devices.

To render the discussion more quantitative, an electric field strength will be considered high if above 200 Td (typical RPC [1–3] operating fields are around 500 Td while typical gaseous microstructure detectors [4] amplification fields are around 200–400 Td). They can conveniently be reached in cylindrical geometries. Indeed several measurements of swarm parameters in avalanche mode exist with such setups, mostly for Ar based mixtures. However, local wire charge up effects [5] or the non-uniformity of the electric field, even over one electron mean free path [6], render the interpretation of such data quite controversial. The possible presence of a non-stationary condition in the swarm development complicates even more the interpretation [7,8]. The cleanest way to avoid such difficulties is, of course, to work in parallel plate geometry. Measurements of electron transport parameters in uniform electric fields at comparable values of E/N are routinely performed in plasma and atomic physics [9].

To import the advantage of working in a clean situation for the interpretation of the results in terms of the fundamental processes cross-sections, yet to extend the currently available data to higher electric fields and complex molecular gases, a special chamber has been developed. Closely related work has also been done by other groups [10,11].

* Corresponding author. Av. Lineu Prestes 2242, Cidade Universitária, 05508-000 São Paulo, SP, Brazil. Tel.: +55 11 3133 9830; fax: +55 11 3133 6745.
E-mail address: ccbueno@ipen.br (C.C. Bueno).

0168-9002/$ - see front matter © 2009 Elsevier B.V. All rights reserved.
doi:10.1016/j.nima.2009.11.019

2. Experimental setup

The planar gas gap used in this work was constituted by one 3 mm thick glass plate (anode) with a bulk resistivity of $2 \times 10^{12}\,\Omega$cm and one profiled circular shaped aluminium electrode of 3 cm diameter (cathode). To change the thickness of the gas gap confined by the electrodes, the metallic cathode was mounted on the nose piece face of a heavy duty linear motion micrometer feedthrough (Huntington-2241-2), which provides displacements parallel to the anode plane with absolute position precision of 2 μm. To allow current measurements, the cathode was electrically insulated from the micrometer actuator structure by a Teflon ring.

In order to ensure the electric field uniformity in the gas gap, the inner face of the glass plate (anode), of active area of 5 mm × 5 mm, was lapped to a flatness of about 1 μm and its borders were smoothed to avoid edge effects. The glass plate was glued on a 50 Ω impedance signal pick-up profiled aluminium plate, electrically insulated from the chamber by a 3 mm thick acrylic slab. High voltage ranging up to 6 kV, supplied by FUG (HCN 350-12500), was applied to the aluminium plate via a low-pass filter constituted by two 50 MΩ resistors, connected in series, and a 2 nF capacitor.

The anode assembly was fixed on a circular aluminium plate attached to the flat spindle faces of three micrometer heads (Mitutoyo 189), angularly spaced at 60°. The independent adjustment of each micrometer allowed tilting the surface of the glass plate in order to achieve the electrodes parallelism. Three metallic cylinder heads placed on the top of the aluminium plate defined a reference plane, whose parallelism to the cathode plate could be checked by the electrical continuity method. The assembly of the anode glass plate was made in a way that ensures that its surface is parallel to this reference plane.

The detector and the micrometric motion system were housed inside a gas-tight stainless-steel chamber (7600 cm^3) provided with quartz windows for the entrance of the UV photons.

Nitrogen or Isobutane gases with purities of 99.999% and 99.9%, respectively, flew continuously through the chamber at a gas flow rate close to 10 cm^3/min. All measurements were performed with gas gaps of 0.5 and 1.0 mm, at atmospheric pressure and at room temperature. Further details about the detector construction are schematically shown in Fig. 1. A photo of the full chamber is shown in Fig. 2.

Measurements were carried out with a nitrogen laser beam (OBB, Mod. GL 3300) focused by a cylindrical lens directly onto the metallic cathode to release photoelectrons from it. The laser delivered pulses at 337 nm wavelength, approximately 1 ns width (manufacturer data), with a repetition rate ranging from 1 up to 20 Hz. At a rate of 5 Hz, the peak power was about 1.45 MW (1.45 mJ per pulse), what required the use of several optical attenuators to reduce the light intensity, mainly at high electric field strengths (i.e. high gas gains).

The anode signal was fed, through a high-voltage decoupling capacitor of 2 nF, to a fast amplifier with 3 GHz bandwidth. The amplifier output and the pulse intensity from the laser, sensed by a photodiode, were digitised by a 1 GHz bandwidth, 10 GS/s sampling rate, Tektronix TDS 7104 oscilloscope.

Independent measurements of the average current induced on the cathode were performed with an electrometer custom-made from a commercially available integrated circuit.

The laser beam was attenuated in tandem by a stepwise progressive and a fixed neutral filter. The progressive filter was adjusted to keep the signal intensity within the electronics linear range as the gas gain was increased. All data points were taken both with and without the fixed filter (attenuation close to 50%)

Fig. 2. View of the open chamber (without the anode assembly). Note the three micrometre heads supporting the anode assembly on the left and the heavy duty linear micrometre holding the cathode on the right. The high voltage feedthrough is also visible in the lower left corner.

A – MITUTOYO 189 micrometer shafts
B – Huntington-2241-2 micrometer shaft
C – Insulating rings
D – Anode support plate
E – Cathode plate
F – Metallic pillars
G – Anode glass plate
H – Insulating foil
I – Aluminium signal pickup electrode
J – Height-adjusting glue layer
K – Acrylic slab
L – Signal cable
M – Coupling capacitor
N – Current-measurement cable

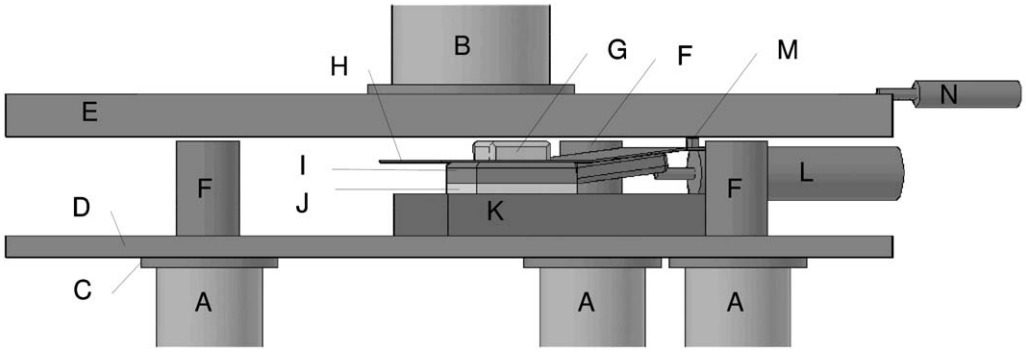

Fig. 1. Schematic drawing of the chamber viewed from top.

and the linearity of the response of the system, which includes possible space–charge effects in the avalanche, was checked.

Both the oscilloscope and the electrometer were controlled by a semi-automatic acquisition chain developed using MATLAB® programming tools.

3. Pulse shape analysis

The determination of electron transport parameters from the transients induced by a swarm developing between parallel plate electrodes is a classic technique, the so-called Pulsed Townsend discharge, well described in the book by Huxley and Crompton [9]. It would be outside the scope of the present paper to review the original works and the later developments, reference will be made only to publications of direct relevance for the current discussion. In general, at high field strengths, attention must be paid to the details of the experimental method to establish a meaningful comparison with numerical calculations solving the Boltzmann transport equation, in particular concerning the drift velocity, as has been demonstrated in a classical series of articles by Sakai and Tagashira [12,13]. However, in this commissioning phase of the setup, the collected data were limited at $E/N \approx 200$ Td, where it has been verified by means of Magboltz simulations (see next section) that differences between the various definitions of drift velocity and between the ionization rate and αv_d are not important [14]. The opposite conclusion is true [14], if the E/N range is extended to ≈ 400 Td. In this work, the distinction between the various definitions of the drift velocity will be ignored, generically employing the symbol v_d, and it will be assumed that $R_i = \alpha\, v_d$.

The study of electron swarm growth in uniform fields is a well advanced topic. In particular, the evolution of the electron density can be calculated analytically including diffusion [9] provided that: any effect of space charge is absent; the hydrodynamic regime is assumed and the time development of the initial ionization is approximated by a Dirac-δ function. To represent the experimental conditions, the effect of the electrodes shall be added. If they are idealised as perfectly absorbing, the correct expression for the electron density evolution contains a series of image charges which is truncated [9]. For this reason, the boundary conditions can only be included approximately at the cathode. On the other hand, those boundary conditions can be included exactly at the anode - the most important ones. The induced current pulse shape can be calculated analytically [9,15]. Of course, it depends on R_i, v_d and the longitudinal diffusion coefficient D_L. It has been verified that such analytical expression agrees well with the numerical solution of the electron continuity equation employing a finite difference scheme similar to that of de Urquijo et al. [16].

Ideally, the analytical expression for the induced current pulse could be fitted to the measured data and the transport parameters extracted. In practise, other experimental effects still prevent this procedure in the present installation of the setup. Most notably, the initial ionization pulse is not a Dirac-δ, but has, on the contrary, a width that is not negligible as compared to the total duration of the signal, especially at the highest field strengths. The start signal, derived as described earlier, also contributes to some jitter. Additionally, some difficulties in focusing the beam onto the cathode may have lead to the extraction of electrons in regions where the field is not uniform. All three effects contribute to a blurring of the theoretical signal shape. For this reason, a simplified approach has been followed in the present initial phase of the setup commissioning: the fitted function is just the convolution of an exponential growth, with rate R_i and in a time window from 0 to $w = d/v_d$, where d is the gap thickness, with a Gaussian of standard deviation σ,

$$f(t) = \frac{1}{2}\exp\left(\frac{\sigma^2 R_i^2}{2}\right) e^{R_i t}\left[\mathrm{erf}\left(\frac{t}{\sqrt{2}\sigma} + \frac{\sigma R_i}{\sqrt{2}}\right) - \mathrm{erf}\left(\frac{t-w}{\sqrt{2}\sigma} + \frac{\sigma R_i}{\sqrt{2}}\right)\right] \quad (1)$$

where $\mathrm{erf}(x) = 2/\sqrt{\pi}\int_0^x \exp(-t^2)\,dt$ is the Error Function. The free parameters are w, R_i, σ plus a global offset and normalisation.

The fit to data taken with Nitrogen at atmospheric pressure and at electric field strengths of $E/N = 61$ Td (no gain, i.e. $R_i = 0$) and $E/N = 143$ Td (with gain, i.e. $R_i \neq 0$) are reproduced in Figs. 3 and 4 (thick curves), respectively. The displayed points are actually an average over 300 waveforms. The statistical errors on both time and voltage are hence reduced to a magnitude smaller than the size of the symbols and they are not reproduced in the figures. The effect of the convolution with a Gaussian (difference between the dashed and the continuous lines) cannot be neglected, especially at the highest E/N. Again, it should be kept in mind that the σ of the Gaussian is a free parameter. It turns out to be independent of the actual voltage (within 25%) and around 1 ns.

To check the validity of the approximation contained in Eq. (1), the values of R_i and v_d, as given by the fit with Eq. (1) and supplemented by a calculation of D_L with the Magboltz program, have been employed to compute the induced current pulse from

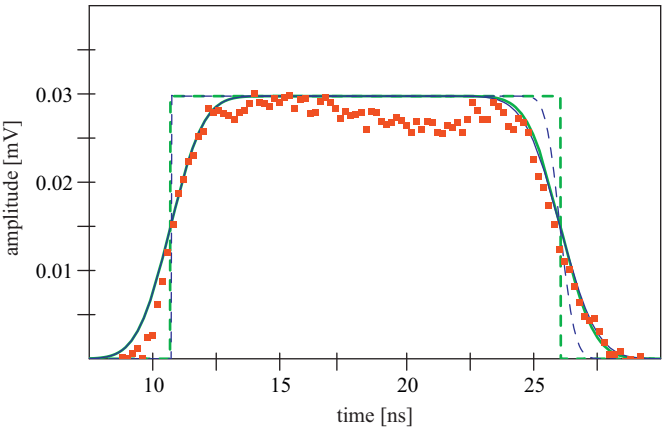

Fig. 3. (Colour online) Pulse shape (average of 300 waveforms) recorded in Nitrogen at room temperature and pressure with 15 kV on a gap of 1 mm ($E/N = 61$ Td). The continuous thick (green online) line is the fit with Eq. (1), which neglects diffusion. The dashed thick (green online) curve shows the corresponding pulse before convolution with a Gaussian apparatus response. The thin (blue online) lines use the same parameter set as the thick ones, but now include the longitudinal diffusion as calculated by the Magboltz code.

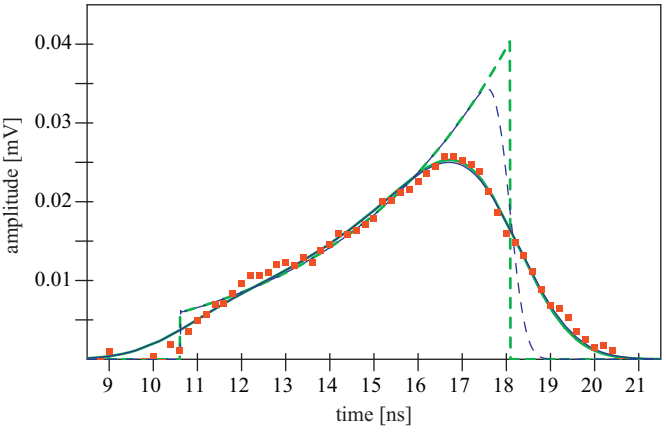

Fig. 4. (Colour online) Same as Fig. 3 but for 35 kV ($E/N = 143$ Td).

the full analytical result mentioned in the beginning, which is also reproduced in Figs. 3 and 4 (thin curves) before and after the convolution with a Gaussian, whose standard deviation is given by the fit with Eq. (1) too. In the end, the result is very close to that using directly Eq. (1), thus justifying the present simplified procedure, but unfortunately, excluding any sensitivity to the value of D_L. A separate systematic study has shown that Magboltz reproduces quite well the available data for all transport parameters in Nitrogen including D_L and D_T [14].

Once proven correct, the simplest fit with Eq. (1) has been applied to all the recorded signals and used to derive the transport parameters. As said earlier, each fitted signal is actually the average of 300 independent waveforms (time aligned). The limitation in going to higher field strengths, apart from discharges in the chamber, is the sensitivity to the shape of the intrinsic pulse once its width becomes comparable to the σ of the Gaussian representing the blurring by the experimental apparatus. When the quality of the fit started to degrade, the analysis has been stopped and higher field strengths were disregarded.

4. Results and discussion

To verify the working condition of the experimental apparatus and the adopted analysis procedure, data were collected with Nitrogen mostly because it is available in high purity grade and it is well known due to a very extensive experimental effort undertaken by several groups over the past 50 years. Finally, chiefly as a result of investigations by Pitchford and Phelps [17], a generally accepted cross-section set has been extracted from the data and can be used in electron transport calculations.

To solve numerically the Boltzmann transport equation for the electrons, the Magboltz [18] code, written by Biagi, has been employed mostly because it is very popular in the particle detector community. Magboltz 1 [19,20], the first generation code by Biagi, employed a semi-analytic approach, consisting in the well known two terms expansion for the electrons velocity distribution function. Magboltz 2 [21] is based on a Monte Carlo integration of the electrons velocity distribution function avoiding the two terms expansion of Magboltz 1 and is hence particularly appropriate to simulate conditions where non-parallel electric and magnetic fields are present, like drift chambers. The energy distribution of the generated electrons after an ionising collision is parametrised with the Opal et al. [22] form, taking their values of the numerical constants. For the present study, both isotropic and non-isotropic versions of the cross-sections set from Pitchford and Phelps has been tried, the change in the results are small in the present range of field strengths. An extensive comparison of the transport parameters calculated by Magboltz 2 versions 2.10, 5.01, 7.01, 8.6 and Imonte version 4.5 has been done [14], but since no appreciable difference has been found in the present E/N range, only Magboltz 2 version 8.6 is reproduced in the present section with the most recent cross-section set `'N2 2008 ANISO'` and the default choice for the parametrisation of the cross-section anisotropies by Okhrimovskyy et al. [23] (dashed curve).

The measured drift velocity (squares) is shown in Fig. 5. The run was performed at room temperature and pressure with a gap of 1 mm. The lower scale gives E/N so that this representation does not change with the working pressure or temperature. The upper scale gives E in the more familiar units of kV/cm assuming a temperature of $T=300$ K and a pressure of 1 atm (the same is true for the secondary scales of all the following figures). The statistical uncertainty is smaller then the size of the symbols. The displayed error bars are systematic only and represent a maximum deviation (10%) estimated by comparing the results obtained in several runs after refocusing the laser and also those collected

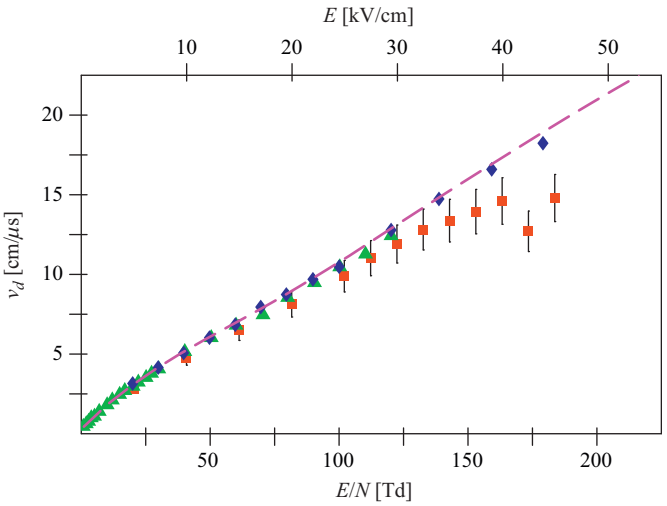

Fig. 5. (Colour online) Measured drift velocity in Nitrogen (squares). The error bars are systematic only. For comparison the data of Purdie and Fletcher [15] (triangles) and Hasegawa et al. [24] (diamonds) are also shown. The dashed line is the Magboltz 2 version 8.6 calculation.

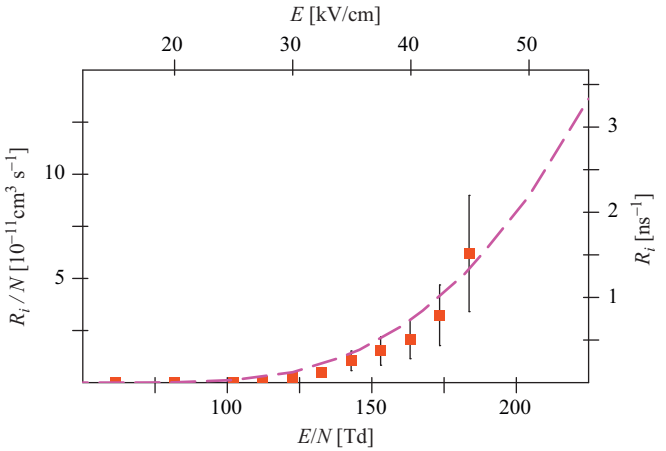

Fig. 6. (Colour online) Measured ionization rate in Nitrogen (squares). The error bars are systematic only. The dashed line is the Magboltz 2 version 8.6 calculation.

with a gap of 0.5 mm. This is likely connected to a residual non-uniformity of the electric field inside the gap. The instability of the fit, visible in the two last points at the highest filed strengths, is originated, as mentioned, by the shortening of the pulse, which becomes comparable with the width of the Gaussian representing the response of the experimental apparatus. For comparison, the results by Purdie and Fletcher [15] (triangles), obtained with a pulse analysis, at lower pressures, have been added. The data of Hasegawa et al. [24] (diamonds) have also been included, although derived with a different method, to cover all the E/N range of the present measurements. The Magboltz calculations agree well with the experimental points.

The ionization rate corresponding to Fig. 5 is displayed in Fig. 6. It should be noted that R_i/N as a function of E/N is a pressure and temperature independent representation. To help the reader, the more familiar R_i and E are also given with secondary scales assuming $T=300$ K and $p=1$ atm. Again, statistical errors are smaller than the symbol size and the bars represent systematic errors only (45%), estimated in the same way as in Fig. 5. Beyond being the only defined physical quantity in a Pulsed Townsend condition rather than α, the ionization rate is

almost uncorrelated with the drift velocity at the data analysis level. Nevertheless, to compare with the other published data, the α values calculated by R_i/v_d from Figs. 5 and 6 are shown in Fig. 7. The error bars (systematic only) represent just the sum of the contributions associated to v_d and R_i, in the same spirit of giving the maximum uncertainty. The data of Daniel and Harris [25] (triangles) and Folkard and Haydon [26] (dots) are considered together with those by Purdie and Fletcher (diamonds) in Fig. 7. The method of Purdie and Fletcher, as noted, is also based on an analysis of the transients in a Pulsed Townsend condition, while Daniel and Harris and Folkard and Haydon have measured α in a columnar discharge. However, there is a good agreement between their results and Magboltz predictions, confirming that such distinctions are not yet important in the present E/N range. Concerning the dataset obtained with the present setup, there might seem to be a tendency to overestimate α for the last two points at the highest E/N. In reality, close examination of Fig. 5 and 6 reveals that it is just originated by the underestimation of the drift velocity for the already mentioned reason. This also illustrates why R_i is a better quantity (i.e. less correlated with v_d) than α to be used in the current method.

Being the quality of the validation with Nitrogen rather satisfactory, data for Isobutane have also been collected. The analysis procedure was the same employed for Nitrogen and the investigation of the systematic errors has shown typically similar values. The run was performed at room temperature and atmospheric pressure, with a gap of 1 mm.

The results for the drift velocity are shown in Figs. 8 and 9 (squares) with an expanded view allowing a comparison among the available accurate data obtained by Gee et al. [27] (crosses), by Breskin et al. [28] (diamonds), by Schmidt [29] (triangles) and by Floriano et al. [30] (dots). The agreement between the measurements taken with the current setup and the others is quite good as well as with the Magboltz calculation (`'ISOBUTANE 2009A'` anisotropic cross-section set). It should be appreciated that a commonly accepted cross-section set for Isobutane does not exist. In fact, those reported here are the first measurements spanning over a significant range of electric field strengths. The correctness of the Magboltz result is then even of more worth. Note that since v_d is smaller in Isobutane, as compared to Nitrogen, the width of the intrinsic pulse is never close to the width of the time response of the system.

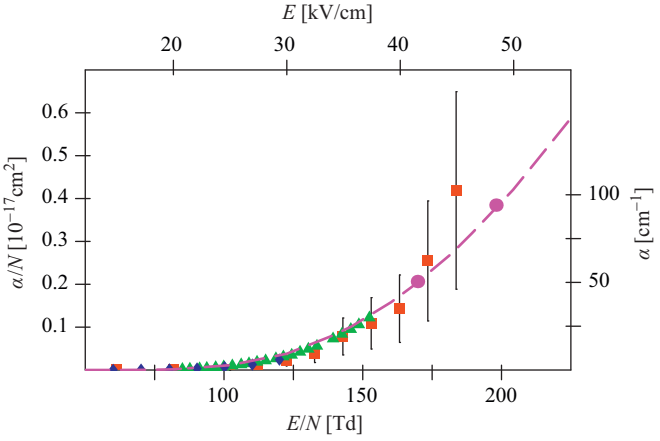

Fig. 7. (Colour online) Calculated first Townsend coefficient $\alpha = R_i/v_d$ in Nitrogen (squares). The error bars are systematic only and have been obtained adding the contributions from Figs. 5 and 6. For comparison the data of Daniel and Harris [25] (triangles), Purdie and Fletcher (diamonds), Folkard and Haydon [26] (dots) have also been included. The dashed line is the Magboltz 2 version 8.6 calculation.

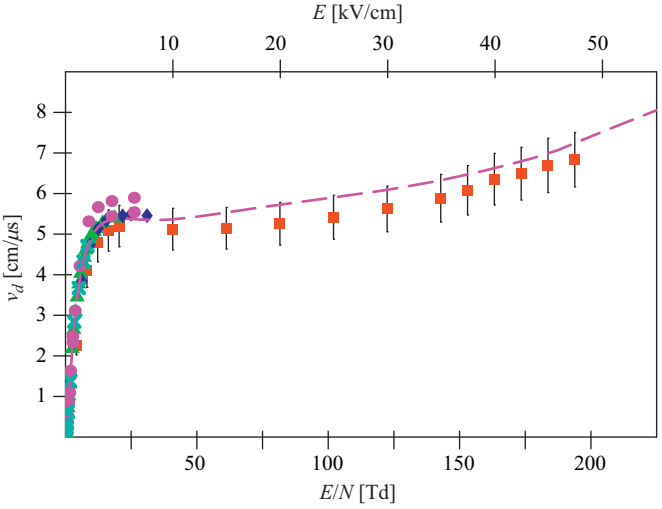

Fig. 8. (Colour online) Measured drift velocity in Isobutane (squares). The error bars are systematic only. For comparison the data of Gee et al. [27] (crosses), Breskin et al. [28] (diamonds), Schmidt [29] (triangles) and Floriano et al. [30] (dots) are also shown. The dashed line is the Magboltz 2 version 8.6 calculation.

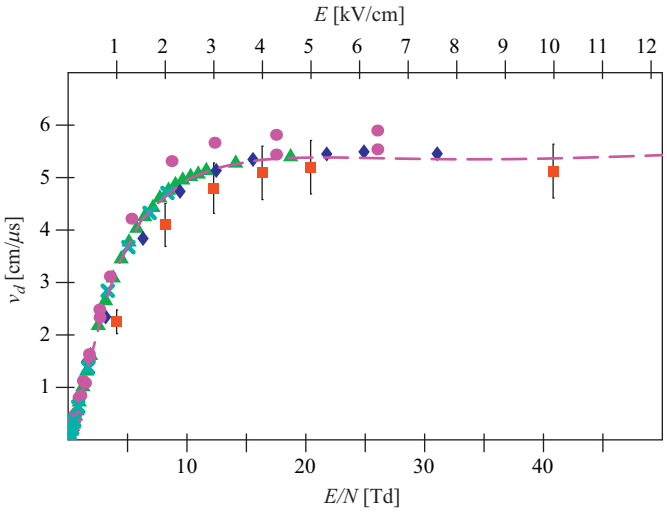

Fig. 9. (Colour online) Enlarged view of Fig. 8 showing the saturation region in detail.

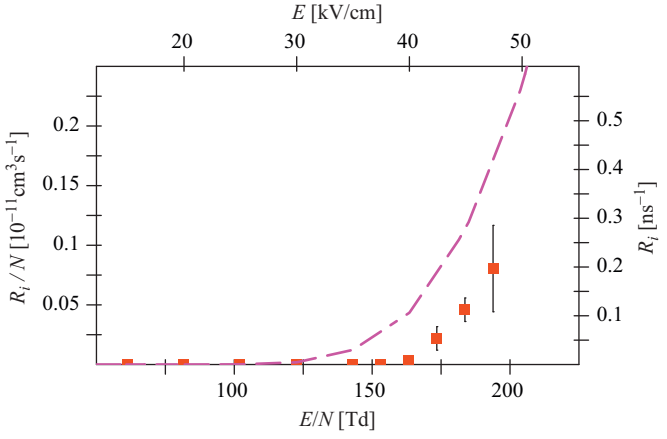

Fig. 10. (Colour online) Measured ionization rate in Isobutane (squares). The error bars are systematic only. The dashed line is the Magboltz 2 version 8.6 calculation.

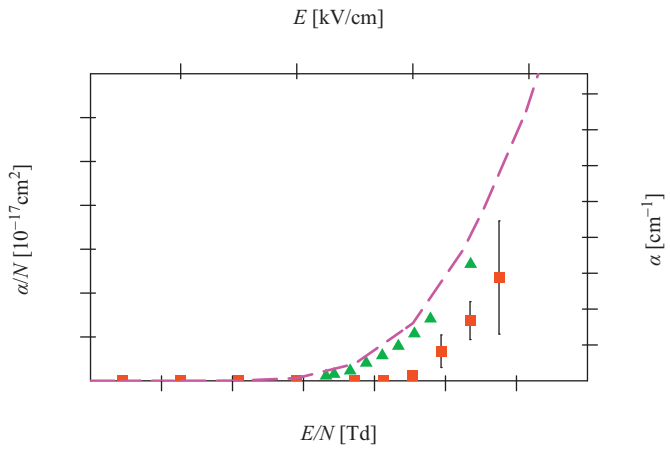

Fig. 11. (Colour online) Calculated first Townsend coefficient $\alpha = R_i/v_d$ in Isobutane (squares). The error bars are systematic only and have been obtained adding the contributions from Figs. 8 and 10. For comparison the data of Heylen for Butane [31] (triangles), have also been included. The dashed line is the Magboltz 2 version 8.6 calculation.

The results for the ionization rate R_i presented in Fig. 10 do not agree with Magboltz calculations. No experimental dataset is available for α in the E/N range considered here, for sake of comparison, Fig. 10 displays the measurements performed in a columnar discharge by Heylen for Butane [31] (triangles). When the present v_d and R_i are used to calculate α (squares), the values do not agree with the Magboltz code. The most likely origin of this discrepancy is the extraction of electrons from regions with reduced electric field strengths. When the gap is small, the laser beam must enter it under a considerable inclination angle and the pulse shape is very sensitive to small movements. Such a peculiar feature has been profited to perform the initial alignment and focusing of the laser beam by selecting a point that yields a clean rectangular signal in ionization mode. However, due to the saturation of the drift velocity in Isobutane, the sensitivity is partially lost rendering the adjustment of the setup more difficult.

5. Conclusions

The newly developed system for measuring electron transport parameters in parallel geometry, high fields and atmospheric pressure performed well in the commissioning phase with Nitrogen, reproducing published data and numerical calculations. New data were collected for Isobutane extending substantially the electric field strengths over which the drift velocity is known, also comparing well with calculations (Fig. 11).

Data on the first Townsend coefficient in Isobutane has been also gathered. However, they disagree with calculations, probably suffering from a laser misfocusing effect. Efforts are under way to correct this problem in a forthcoming paper. The possibility to gain experimental sensitivity to the longitudinal diffusion is not excluded.

The duration of the laser pulse, probably due to the characteristics of the specific laser model employed, limits the highest usable field strength for fast gases like Nitrogen. Its origin will be investigated further.

Finally, the chamber has been designed to operate at lower pressures, but this possibility has not been explored, for the moment, due to the lack of needed ancillary equipment.

Acknowledgements

The authors gratefully acknowledge Dr. M.M.R. Fraga for helpful discussions on the meaning of electron transport parameters at high field strengths. They are in debt to her profound knowledge of the methods to solve numerically the Boltzmann transport equation. They also thank Dr. Jiro Takahashi (IFUSP) for the precision mechanical work necessary in the chamber construction, A.M.A. Pereira for assistance with the gas distribution system and N.M.V.C. Carolino and O.L. Cunha for helping with the read-out and control electronics. This work was co-financed by FAPESP under Contract 02/04697-1 and by FCT, EU, FEDER and POCI via Contract POCI/FP/81981/2007. Two of the authors (SB and AM) acknowledge a fellowship from FAPESP under Contract 06/58855-8 and 07/50591-4, respectively.

References

[1] R. Santonico, R. Cardarelli, Nucl. Instr. and Meth. A 187 (1981) 377.
[2] R. Santonico, R. Cardarelli, A.D. Biagio, A. Lucci, Nucl. Instr. and Meth. A 263 (1988) 20.
[3] P. Fonte, R. Ferreira-Marques, J. Pinhão, N. Carolino, A. Policarpo, Nucl. Instr. and Meth. A 449 (2000) 295.
[4] A. Oed, Nucl. Instr. and Meth. A 263 (1988) 351.
[5] E. de Lima, M. Salete, S.C.P. Leite, A.J.P.L. Policarpo, M.A.F. Alves, IEEE Trans. Nucl. Sci. NS-31 (1984) 94.
[6] J. Miyamoto, G.F. Knoll, Nucl. Instr. and Meth. A 399 (1997) 85.
[7] H. Sakurai, B.D. Ramsey, Nucl. Instr. and Meth. A 313 (1992) 155.
[8] I.K. Bronić, B. Grosswendt, Nucl. Instr. and Meth. B 142 (1998) 219.
[9] L.G.H. Huxley, R.W. Crompton, The Diffusion and Drift of Electrons in Gases, Wiley, New York, 1974.
[10] P. Colas, A. Delbart, J. Derré, I. Giomataris, F. Jeanneau, V. Lepeltier, I. Papadopoulos, P. Rebourgeard, Nucl. Instr. and Meth. A 478 (2002) 215.
[11] G. Chiodini, M. Colucci, E. Gorini, M. Primavera, S. Stella, Nucl. Phys. B (Proc. Suppl.) (2006) 133.
[12] Y. Sakai, H. Tagashira, S. Sakamoto, J. Phys. D 10 (1977) 1035.
[13] H. Tagashira, Y. Sakai, S. Sakamoto, J. Phys. D 10 (1977) 1051.
[14] A. Mangiarotti, A theoretical study of the fast signal induced by avalanche growth in pure Nitrogen and pure Isobutane, Activity Report of Project FAPESP 07/50591–4.
[15] P.H. Purdie, J. Fletcher, J. Phys. D 22 (1989) 759.
[16] J. de Urquijo, A.M. Juarez, J.C. Rodríguez-Luna, J.S. Ramos-Salas, IEEE Trans. Plasma Sci. 35 (2007) 1204.
[17] A.V. Phelps, L.C. Pitchford, Phys. Rev. A 31 (1985) 2932.
[18] S. Biagi, Magboltz, The Fortran source code of the stand alone version is freely downloadable from ⟨http://consult.cern.ch/writeup/magboltz/⟩, 2007.
[19] S. Biagi, Nucl. Instr. and Meth. A 273 (1988) 533.
[20] S. Biagi, Nucl. Instr. and Meth. A 283 (1989) 716.
[21] S. Biagi, Nucl. Instr. and Meth. A 421 (1999) 234.
[22] C.B. Opal, W.K. Peterson, E.C. Beaty, J. Phys. Chem. 55 (1971) 4100.
[23] A. Okhrimovskyy, A. Bogaerts, R. Gijbels, Phys. Rep. 65 (2002) 037402.
[24] H. Hasegawa, H. Date, M. Shimozuma, K. Yoshida, H. Tagashira, J. Phys. D 29 (1996) 2664.
[25] T.N. Daniel, F.M. Harris, J. Phys. B 3 (1970) 363.
[26] M.A. Folkard, S.C. Haydon, J. Phys. B 6 (1973) 214.
[27] N. Gee, G.R. Freeman, Radiat. Phys. Chem. 15 (1980) 267.
[28] A. Breskin, R. Chechik, Nucl. Instr. and Meth. A 252 (1986) 488.
[29] B. Schmidt, Nucl. Instr. and Meth. A 252 (1986) 579.
[30] M.A. Floriano, N. Gee, G.R. Freeman, J. Phys. Chem. 84 (1986) 6799.
[31] A.E.D. Heylen, Int. J. Electr. 39 (1975) 653.